Hindawi
Science and Technology of Nuclear Installations
Volume 2022, Article ID 2822857, 8 pages
https://doi.org/10.1155/2022/2822857

Research Article

Oceanic Radionuclide Dispersion Method Investigation for Nonfixed Source from Marine Reactor Accident

Dingqing Guo[1,2] **Jinkai Wang**[1] **Daochuan Ge**[3] **Chunhua Chen**[3] **and Liwei Chen**[4]

[1]*State Key Laboratory of Nuclear Power Safety Monitoring Technology and Equipment, China Nuclear Power Engineering Co., Ltd., Shenzhen 518172, China*
[2]*School of Mechanical Engineering, Shanghai Jiao Tong University, Shanghai 200240, China*
[3]*Institute of Nuclear Energy Safety Technology, Hefei Institutes of Physical Science, Chinese Academy of Sciences, Hefei, Anhui 230031, China*
[4]*School of Computer Science and Technology, Hefei Normal University, Hefei, Anhui 230601, China*

Correspondence should be addressed to Daochuan Ge; daochuan.ge@inest.cas.cn and Chunhua Chen; chunhua.chen@inest.cas.cn

Received 3 January 2022; Accepted 16 March 2022; Published 18 April 2022

Academic Editor: Peter Ivanov

Radionuclide dispersion model, which is of critical importance to the emergency response of severe nuclear accident, is used to estimate the consequences arising from accidental or routine releases and to predict areas of high contamination. It is difficult to evaluate the radioactive consequence accurately and rapidly for the accidental release of radionuclides from marine reactor because of the complex mobility feature in the sea. Based on CFD method, a finite-volume, three-dimensional regional oceanic dispersion model was developed in this paper to simulate the dispersion of radionuclides originating from marine reactor. The simulated dose variation of 137Cs presented good agreement with the monitoring data of marine radioactive pollution caused by Fukushima Dai-ichi nuclear accident, which demonstrated the validity of the method. A severe accident scenario of marine reactor was simulated and analyzed, which indicates that the regional oceanic dispersion model can provide dose assessment for nuclear emergency response.

1. Introduction

The marine reactor, equipped in the offshore mobile platform, is used to provide nuclear propulsion (e.g., the nuclear-powered icebreaker and nuclear merchant ship) or electrical supply (e.g., the floating nuclear power plant, FNPP). Since the first nuclear submarine put into service in 1955, some 700 marine reactors have served at sea on various vessels worldwide and about 200 marine reactors are still in operation [1]. However, risks of accidents caused by extreme events such as storms, tsunamis, flooding, and collisions are unavoidable safety concerns to marine reactors. Differed from the land-based nuclear power plant, the marine reactor always experiences the effects of ship motions or load variation due to sea condition [2], which results in greater accident probability. There have been many emergencies and incidents in the history. From 1959 to 2007, Russian nuclear-powered submarines occurred 165 safety-related events [3]. In 1985, the submarine K431 was being refueled when a spontaneous chain reaction occurred [4], which resulted in violent explosion and radioactive contamination over a significant area in Chazhma Bay [5]. Though no indications of leakage have been observed from the sunken submarines Komsomolets [6, 7] and Kursk [8], the public are acutely sensitive to the potential long-term risks of contamination. The worst accidents, which always caused international disputes, were accompanied by serious ecological and radiological hazards.

Nowadays, 95% of global goods are moved by shipping [1]. Meanwhile, shipping contributes about 7% of the anthropogenic SO_2 emissions and 15% of the NOx emissions [9]. Nuclear propulsion is the only proven emissions-free option prone to substitute conventional ship propulsion [10, 11]. In future, the application of marine nuclear propulsion would become more widespread because of the constraints on fossil fuel use in transport [12]. As an economical solution to drive development in remote but resource rich areas such as the Arctic, the first FNPP, Academician Lomonosov, is expected to be delivered to Russia in 2019 [13]. China will prioritize the development of FNPPs in the coming five years to support offshore oil and gas exploitation in the South China Sea [14]. All of them would increase the risk of radionuclides release from marine reactors to ocean, consequently.

Marine dispersion model plays a major role in obtaining emergency decision to minimize the potential hazards to humans and the environment and can serve for further dose assessments. Environmental Modeling for Radiation Safety (EMRAS) project [15], organized by the International Atomic Energy Agency (IAEA) from 2003 to 2007, included a working group on model validation for radionuclides transport in watershed river and estuarine systems. The working group studied five scenarios in aquatic systems [16], but without any marine environment consideration. In the subsequent EMRAS II program (from 2009 to 2011), even no specific working group for the aquatic system was included [17]. The Fukushima Dai-ichi accident, which caused serious marine pollution, has largely reinforced the development of marine nuclear emergency capabilities, and since 2011, a significant number of radionuclide dispersion models have been published. Kawamura et al. [18] applied the particle random-walk model SEA-GEARN to simulate the oceanic spreading of 131I and 137Cs, which became first studies published after the accident. Miyazawa et al. [19] developed a dispersion model of 137Cs based on an Eulerian transport equation. A high-resolution (1 km) regional ocean model was used to simulate the 137Cs concentration from March to May by Tsumune et al. [20]. More recently, a comprehensive intercomparison of marine dispersion models which were applied to the Fukushima Dai-chi nuclear accident were conducted in the frame of MODARIA program by IAEA [21]. At present, the MODARIA II program is being executed, which includes a working group assessing the transportation of radionuclides released in the marine environment [22].

When radionuclides released from a nonfixed marine reactor, the short-term, near-range prediction of marine radioactivity dispersion is urgent and meaningful for emergency response at the early stage of accident. It helps the rescuers to reduce or even avoid the radiation exposure with an accurate prediction of the near-range radionuclide distribution around the marine reactor under accident. However, the significant uncertainty of the accident region makes it difficult to implement rapid direct monitoring. Though there have been many marine dispersion models, most of them are (1) used for the long-term, large-scale prediction [23] and (2) applied to predict the release from fixed source (e.g., coastal nuclear power plant), not optimized for the mobile platform [21].

Compared with the existing models, computational fluid dynamics (CFD) approaches, which are particularly useful when modeling pollutant dispersion on complex terrain [24], offer a large potential to increase the accuracy of the simulation [25]. The objective of this study was to develop a finite-volume, three-dimensional regional oceanic dispersion model, based on the CFD tools in OpenFOAM [26] package and to simulate the accidental marine dispersion of radionuclides originating from the floating marine reactors accurately and swiftly.

2. Model Description

Apart from the direct discharge of high radioactive liquid wastes to the sea, atmospheric deposition of radionuclides to the sea surface is another pathway from the accident site to the ocean when severe marine reactor accident happens. In this paper, only the direct release is taken into consideration.

The facilities with the marine reactor can be located varying from the offshore waters to the deep ocean. Oceanic dispersion simulations of radionuclides basically consist of a radionuclide dispersion model and an ocean hydrodynamic model [27]. The dispersion model is employed to calculate the movement of radionuclides while the ocean hydrodynamic model is used to model background flow field. In this article, we focus on the radioactive pollutant dispersion at the early stage of accident, namely, a regional small-scale simulation in the short term.

2.1. General Fluid Dynamic Equation. Navier–Stokes equations are applied nowadays to denote collectively the conservation equations of mass, momentum, and energy [28]. CFD approaches, which are capable of modeling small-scale and detailed flow structure, simulate fluid flow by solving the full Navier–Stokes equations [23]. In Cartesian coordinates, the differential form of the generic conservation equation for the transport of a property ϕ is expressed as [29]:

$$\frac{\partial(\rho\phi)}{\partial t} + \frac{\partial(\rho u_j \phi)}{\partial x_j} = \frac{\partial}{\partial x_j}\left(\Gamma \frac{\partial \phi}{\partial x_j}\right) + S_\phi, \qquad (1)$$

where Γ is the generic diffusivity for ϕ and S_ϕ is the generic source or sink of ϕ. Equation (1) describes the nonlinear and coupled governing equations (e.g., momentum, continuity, salinity, and density equations) of fluid flow, which are difficult to solve. In small-scale ocean hydrodynamic model used in this work, the flow field distribution is the main factor affecting the spread of radionuclides and following reasonable assumptions must be made:

(1) Seawater is treated as an incompressible, isothermal, and Newtonian fluid [30]
(2) Radionuclide concentration is considered as a passive scalar, which has no dynamical effect on the seawater motion [31]
(3) Coriolis force is neglected within small-scale
(4) Concentration variations of other solutes are not taken into consideration

The simplified governing equations are sufficient for the description of incompressible, laminar flow; they are still nonlinear and subject to instability [30]. The waters where marine reactors operated are almost always turbulent [32].

Reynolds-averaged approaches to turbulence are introduced to solve the Navier–Stokes equations, which yields the Reynolds-averaged Navier–Stokes (RANS) equations [29].

2.2. Turbulence Model. The standard $k-\varepsilon$ turbulence model [29] is selected to solve the RANS equations. The averaged continuity and momentum equations can be written as,

$$\frac{\partial(\rho\overline{u_i})}{\partial x_i}=0,$$
$$\frac{\partial(\rho\overline{u_i})}{\partial t}+\frac{\partial\left(\rho\overline{u_i u_j}\right)}{\partial x_j}=-\frac{\partial\overline{p}}{\partial x_i}+\frac{\partial}{\partial x_j}\left(\mu\frac{\partial\overline{u_i}}{\partial x_i}-\rho\overline{u_i'u_j'}\right), \quad (2)$$

where ρ is the seawater density, $\overline{u_i}$ is the mean velocity in the x, y, z direction, u_i' is the fluctuating velocity, and μ means the kinematic viscosity of seawater.

To close the equations, a turbulence model is introduced. Assume that the turbulence effect can be described as an increased viscosity, which leads to the eddy-viscosity model for the Reynolds stress:

$$-\rho\overline{u_i'u_j'}=\mu_t\left(\frac{\partial\overline{u_i}}{\partial x_j}+\frac{\partial\overline{u_j}}{\partial x_i}\right)-\frac{2}{3}\rho k\delta_{ij}, \quad (3)$$

and the eddy-diffusion for a scalar:

$$-\rho\overline{u_j'\phi'}=\Gamma_t\frac{\partial\overline{\phi}}{\partial x_j}. \quad (4)$$

In equation (4), k is the turbulent kinetic energy, and δ_{ij} is the Kronecker delta. The eddy-viscosity μ_t can be expressed as,

$$\mu_t=\rho C_\mu\frac{k^2}{\varepsilon}, \quad (5)$$

where ε stands for the turbulent dissipation rate.

The rate of production of turbulence kinetic energy by the mean flow can be written as,

$$P_k=-\rho\overline{u_i'u_j'}\frac{\partial\overline{u_i}}{\partial x_j}\approx\mu_t\frac{\partial\overline{u_i}}{\partial x_j}\left(\frac{\partial\overline{u_i}}{\partial x_j}+\frac{\partial\overline{u_j}}{\partial x_i}\right). \quad (6)$$

The standard $k-\varepsilon$ turbulence model is given by:

$$\rho\frac{\partial k}{\partial t}+\rho\overline{u_j}\frac{\partial k}{\partial x_j}=\frac{\partial}{\partial x_j}\left[\left(\mu+\frac{\mu_t}{\sigma_k}\right)\frac{\partial k}{\partial x_j}\right]+P_k-\rho\varepsilon,$$
$$\rho\frac{\partial\varepsilon}{\partial t}+\rho\overline{u_j}\frac{\partial\varepsilon}{\partial x_j}=\frac{\partial}{\partial x_j}\left[\left(\mu+\frac{\mu_t}{\sigma_\varepsilon}\right)\frac{\partial\varepsilon}{\partial x_j}\right]+C_{\varepsilon1}P_k\frac{\varepsilon}{k}-\rho C_{\varepsilon2}\frac{\varepsilon^2}{k}. \quad (7)$$

This model contains five constant parameters: $C_\mu=0.09$, $C_{\varepsilon1}=1.44$, $C_2=1.92$, $\sigma_k=1.0$, and $\sigma_\varepsilon=1.3$ are the most commonly used values.

2.3. Radionuclide Dispersion Model. The most common marine reactor type is the uranium-fueled pressurized water reactor [1]. Various kinds of radionuclides could be emitted from severe marine reactor accidents, among which 137Cs and 131I are representative of volatile, dissolved fission products [33]. Radionuclide behavior in the marine environment is complicated, and it consists of multiple processes, such as dissolution, precipitation, sorption, and suspension. It is unpractical to integrate all the physical and chemical processes in such a short paper. The influence from sorption, precipitation, and suspension is ignored. Therefore, the dispersion of radionuclide contaminants in the sea are predominantly controlled by two factors [34]:

(1) Transportation by the ocean current
(2) Diffusion caused by the concentration gradient and the turbulence

Turbulent flows are chaotic, diffusive causing rapid mixing. The effective diffusivity in turbulence is at least three orders of magnitude greater than the diffusivity on molecular scale [32]. Consequently, pollutant dispersion, being mainly due to turbulence, is independent of the characteristics of the pollutant itself [34]. In modeling the fluxes of pollutants in coastal waters, the corresponding general solute advection-diffusion equation can be written as,

$$\frac{\partial\rho\overline{C}}{\partial t}+\frac{\partial\left(\rho\overline{u_j C}\right)}{\partial x_j}=\frac{\partial}{\partial x_j}\left(-\rho\overline{u_j'C'}\right)+S_C, \quad (8)$$

$$-\rho\overline{u_j'C'}=\Gamma_C\frac{\partial\overline{C}}{\partial x_j}, \quad (9)$$

where C stands for the radionuclide concentration at point of (x, y, and z) at each time step; Γ_C means the turbulent diffusivity of the radionuclide, which also varies in space and time; and S_C represents the sources in the model.

Decay of radionuclides, described by the radioactive decay constant λ, can be introduced to the advection-diffusion equation by adding the term $-\lambda C$ to the right hand side of equation (9). The relationship between λ and the half-life ($t_{1/2}$) is expressed as the following:

$$\lambda=\frac{\ln 2}{t_{1/2}}. \quad (10)$$

In the following section, the Fukushima nuclear accident data are used to validate the mathematical model mentioned previously. Then, radionuclide dispersion in the open sea was simulated to study spread trend after marine reactor accident.

3. Simulation Configuration

Before the simulation in this case, some configuration in OpenFOAM should be illustrated and explained firstly, which guarantee that the accuracy of simulation. Mesh generation, which impacts substantially on the quality of simulation result, would be the most time-consuming and labor-intensive part in the process of CFD simulation [35]. Consequence assessment in a timely manner is of great importance to nuclear emergency response, which requires fast mesh generation. Automated mesher such as the snappyHexMesh [36], which is part of the OpenFOAM package, has been proved to be sufficiently practical to generate the finite-volume hexahedra meshes. The snappyHexMesh operates an automated and robust meshing process, which is described clearly [35]. The controllable mesh parameters set in the input file can be specified and optimized in advance. When accident happens, snappyHexMesh can generate a high-quality mesh quickly and automatically based on the STL file of the geometry, which can accelerate emergency response. Figure 1 shows a detail of the seabed included in the mesh generated by snappyHexMesh, refined close to the reefs ($<1m$). In order to obtain solutions independent of mesh, several mesh tests were performed.

The pimpleFoam solver has been secondary developed and applied. The inlet velocity is set as 2 m/s along the x direction. Time step is 0.1 s, and the calculation data are resampled each 0.5 s. In Figure 1, the nuclear merchant ship was firstly located at red dot 1 (20, 230, 10). Since 700^{th} s to 800^{th} s, the ship was drifted directly to the red dot 2 (40, 290, 10) gradually with a constant speed; then, the ship was stuck to the seafloor at dot 2. The release rate of 137Cs is set as a constant (1010 Bq/s) throughout the calculation.

4. Typical Marine Reactor Accident Scenario

When radionuclides released from a marine reactor after the severe nuclear accident, it is urgent to assess the radiation distribution quickly, which gives decision support in emergency rescue to minimize the potential hazards. A hypothetical accident scenario was set to investigate the radionuclides dispersion on the complex seafloor with irregular reefs.

4.1. Accident Scenario Description. The assumed accident is described as following: a nuclear merchant ship loading heavy freight encountered a fierce storm causing navigation system failure. The ship sunk to the seafloor after striking on a rock. The reactor was severely damaged, and radioactivity was detected. The schematic view of the geometric model is showed in Figure 1, and the coordinate origin is represented by a black dot. The seabed is 100 meters under the water. The nuclear merchant ship is noted as a red dot, which is gradually pushed away from point 1 to point 2 by the current. The reefs (denoted from A to G) with a variety of geometries were distributed in the seafloor, which are shown in maroon color. The size of the reefs varies from 50 m (F) to 200 m (G) and the height varies from 15 m (A) to 50 m (G).

4.2. Radionuclide Dispersion. The transportation of radionuclide mainly controlled by the flow of seawater. Figure 2 shows the velocity field around the reefs, which corresponds to a plane of 10 m above the seafloor. The flow field is turbulent and inhomogeneous, and wake flows are generated behind the blunt reefs. A reserve flow region behind the reef G is presented clearly in Figure 2, where the flow is moving toward the reef G.

The distribution of pollutant concentration in vertical plane ($y = 225$) is shown in Figure 3, which demonstrates the moment of 300^{th} s after the accidental release. The process of dispersion from the bottom of the sea to the surface is clear and intuitive.

The flow, which determines the distribution of radionuclides around the reefs, is affected by the size and shape of them. In Figure 3, it is obvious to see that reef A and G with sharp back edges caused a dip of the radionuclide concentration. To have a better understand of the effect of reefs and the process of dispersion, the horizontal distribution at four different moments (100 s, 300 s, 500 s, and 700 s) of radioactive pollutant concentration is shown in Figure 4. 137Cs disperses continuously in temporal and spatial.

The mobility is a significant feature of the marine reactor, which increases the difficulty in assessing the radiation distribution. Since 700^{th} s referring to the initial time of the accident, the nuclear merchant ship drifted to dot 2 within 100 s by the ocean current and after that the ship stuck in the seabed. The changing processes of radionuclide distribution during ($T = 750s$, $T = 800s$) and after (T = 1000 s, T = 1700 s) the motion of the ship are shown in Figure 5.

The concentration at the downstream of the marine reactor changes with the motion of the source. High concentration of 137Cs was diluted gradually by the flush of currents. The process of dilution (from $T = 1000s$ to $T = 1700s$ in Figure 5) is inhomogeneous in temporal and spatial, for the turbulence and vortices in the flow field (see Figure 2).

5. Discussion and Conclusion

A high-resolution, small-scale oceanic dispersion model was developed to simulate the initial spreading of radionuclides discharged from the marine reactor, which is nonfixed and floating in the sea. In this study, given that the close similarity to the marine reactor accident scenario, the direct discharge of highly contaminated water from the 1F NPP reactor was used to validate the reliability and accuracy of the oceanic dispersion model. The results showed that it performs satisfactorily in simulating the distribution of 137Cs in the complex coastal terrain, and the calculation results were in good agreement with the monitoring data. Compared with the observed data, the deviations of the simulated results are mainly from the uncertainties in source estimation, the complexity in boundary conditions, and the omission of absorption by bottom sediments.

A marine reactor accident scenario, accompanied by the moving of radioactive source, was simulated to analyze the dispersion of radionuclides in the irregular ocean floor terrain. High-resolution flow field was generated, which displayed vortices around the reefs. The radionuclide concentration from both fixed source and nonfixed source is calculated. In this paper, the vertical dispersion from the

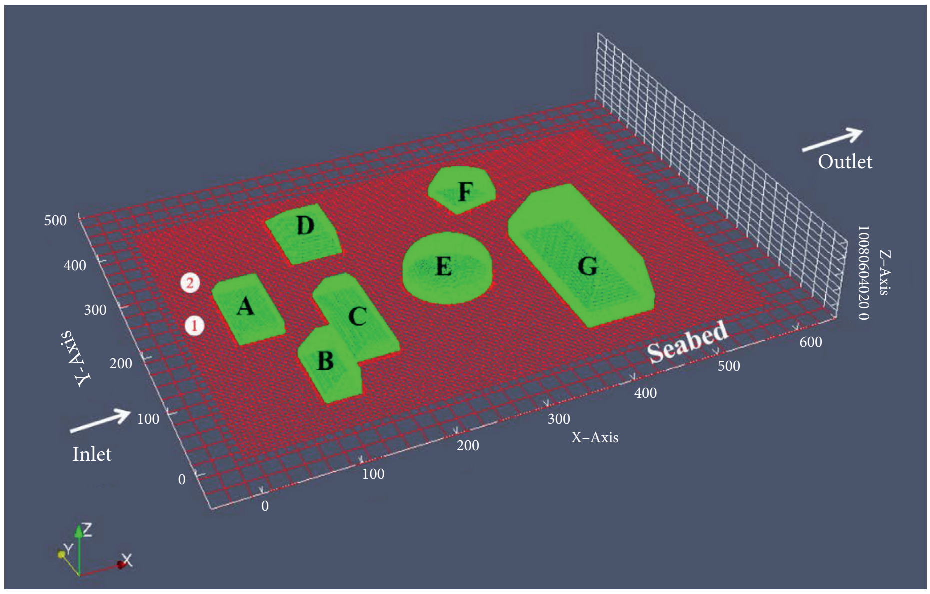

Figure 1: Sunken marine reactor on the seafloor with irregular reefs distribution.

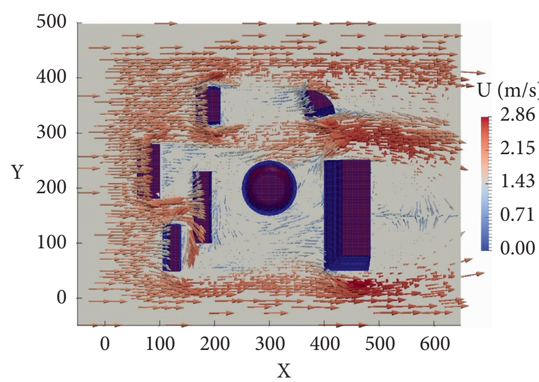

Figure 2: Detailed flow field around the reefs (velocity vectors 15 m above seafloor).

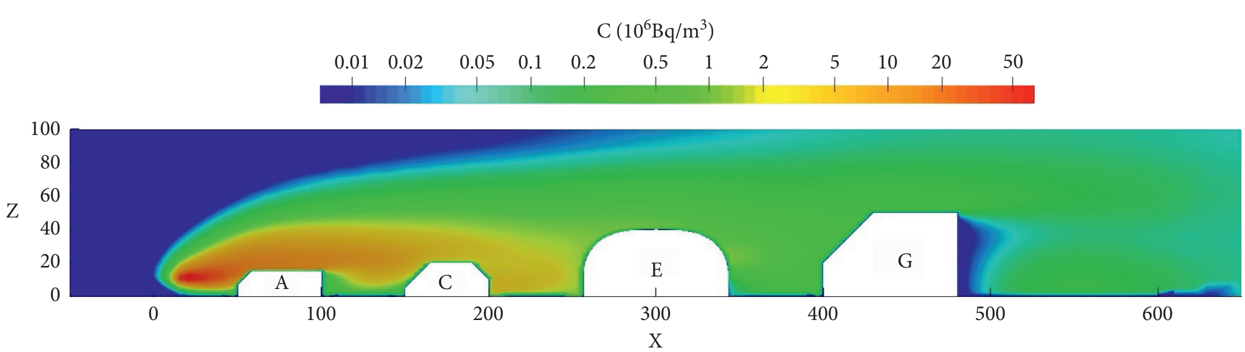

Figure 3: Vertical distribution of radioactive pollutants (in the XZ plane, where $y = 225$ and $T = 300s$).

seabed to the surface and the horizontal distribution of radioactive pollutant released from a fixed source were presented. In addition, the dispersion of radionuclide from nonfixed source was analyzed. It is suggested that the regional radionuclide dispersion model can be used as an important tool to study and predict the oceanic radionuclide dispersion and to provide dose assessment for emergency response. All the simulated results shown an obvious influence of ocean floor terrain to the distribution of the pollutant, which provides a scientific basis for a rapid

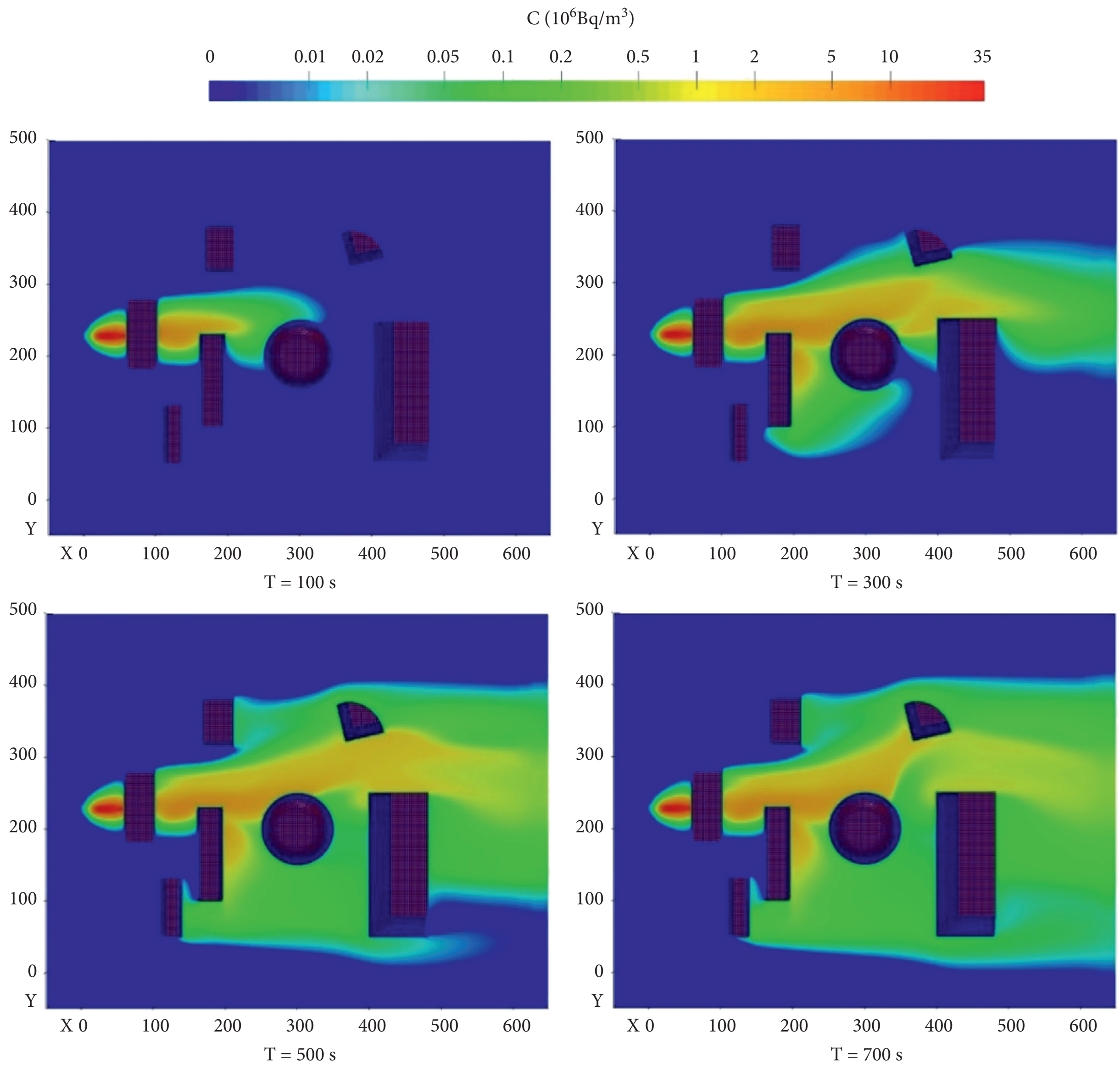

Figure 4: Horizontal distribution of 137Cs concentration at different time (in the XY plane, where $z = 15$).

development of rescue routes under the marine nuclear accident. Especially, the nonfixed source introduced an extrasignificant uncertainty to the monitoring of the radionuclide concentration; the simulation results supply a strong evidence to the decision of nuclear emergency response.

In this study, the processes of sorption, precipitation, and suspension between radionuclides and the environment were not taken into consideration. In addition, the process of current movements caused by winds was ignored. More studies are needed to improve the capability of the regional oceanic dispersion model.

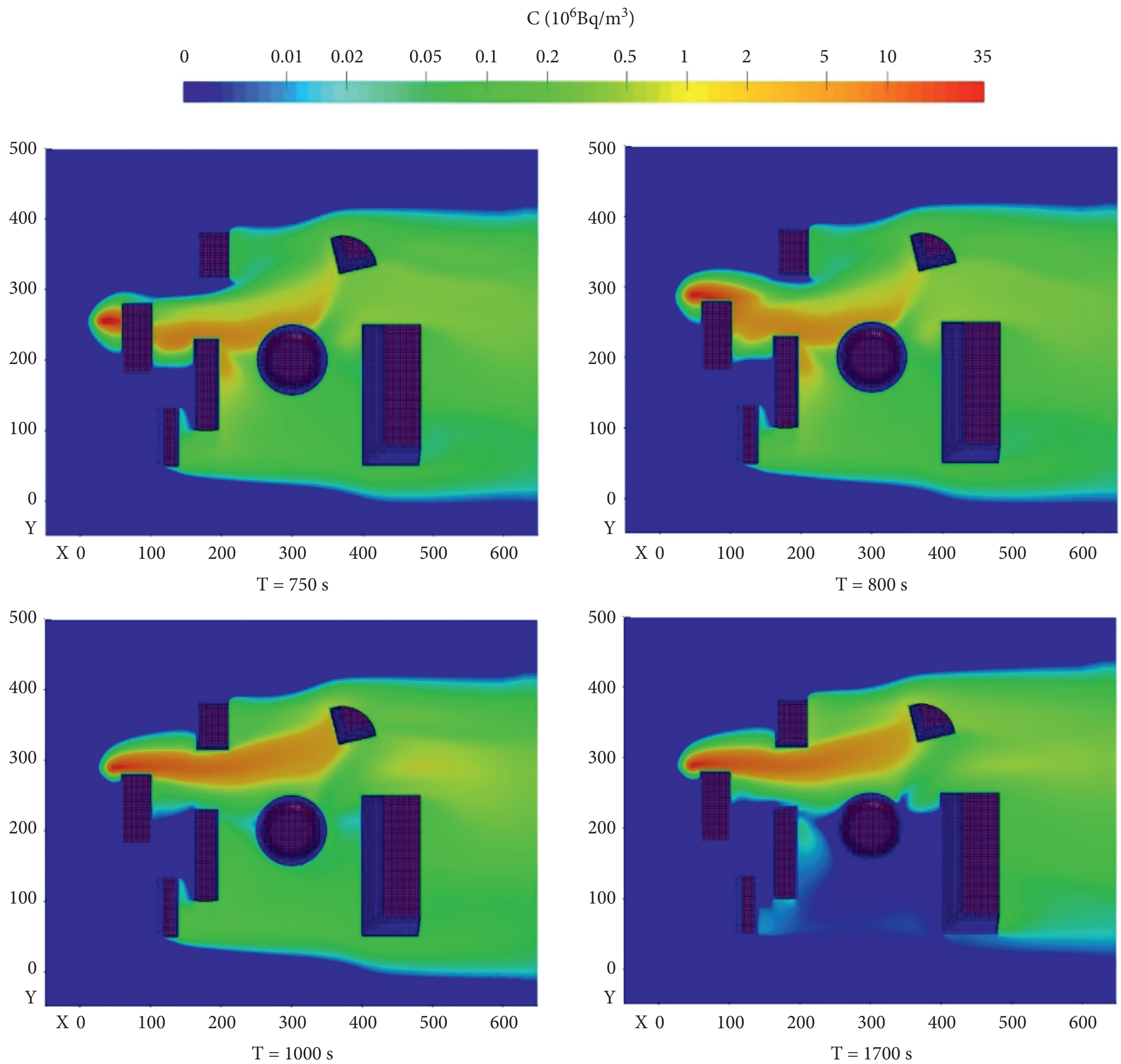

FIGURE 5: Concentration variation of 137Cs with the motion of source (in the XY plane, where z = 15).

Data Availability

No data are available on request.

Conflicts of Interest

The authors declare that they have no conflicts of interest.

Acknowledgments

This work was supported by the Project of Anhui Nuclear Emergency Command Platform Based on Pengze Nuclear Power Plant, the Chinese Academy of Sciences' Defense Science and Technology Innovation Fund (no. CXJJ-17-M175).

References

[1] Royal Academy of Engineering, *Future Ship Powering Options Exploring Alternative Methods of Ship Propulsion*, Royal Academy of Engineering, London, UK, 2013.

[2] T. Ishida, T. Kusunoki, M. Ochiai, T. Yao, and K. Inoue, "Effects by sea wave on thermal hydraulics of marine reactor system," *Journal of Nuclear Science and Technology*, vol. 32, no. 8, pp. 740–751, 1995.

[3] O. Reistad, S. Hustveit, and S. Roudak, "Operational and accident survey of Russian nuclear submarines for risk assessments using statistical models for reliability growth," *Annals of Nuclear Energy*, vol. 35, pp. 2126–2135, 2008.

[4] Y. V. Sivintsev, V. L. Vysotskii, and V. A. Danilyan, "Radioecological consequences of a radiation accident in a nuclear-powered submarine in Chazhma cove," *Atomic Energy*, vol. 76, pp. 157–160, 1994.

[5] W. J. F. Standring, M. Dowdall, I. Amundsen, and P. Strand, "Floating nuclear power plants: potential implications for radioactive pollution of the northern marine environment," *Marine Pollution Bulletin*, vol. 58, pp. 174–178, 2009.

[6] S. Hoibraten, P. E. Thoresen, and A. Haugan, "The sunken nuclear submarine Komsomolets and its effects on the environment," *Science of the Total Environment*, vol. 202, pp. 67–78, 1997.

[7] V. A. Nikolaev, A. V. Gromov, and A. V. Stepanov, "Track detectors in radiation monitoring of the sunken submarine "Komsomolets"," *Radiation Measurements*, vol. 28, pp. 381–384, 1997.

[8] I. Amundsen, M. Iosjpe, O. Reistad et al., "The accidental sinking of the nuclear submarine, the Kursk: monitoring of radioactivity and the preliminary assessment of the potential impact of radioactive releases," *Marine Pollution Bulletin*, vol. 44, no. 6, pp. 459–468, 2002.

[9] J. Beecken, J. Mellqvist, K. Salo et al., "Emission factors of SO_2, NOx and particles from ships in Neva Bay from ground-based and helicopter-borne measurements and AIS-based modeling," *Atmospheric Chemistry and Physics*, vol. 15, no. 9, pp. 5229–5241, 2015.

[10] S. E. Hirdaris, Y. F. Cheng, P. Shallcross et al., "Considerations on the potential use of Nuclear Small Modular Reactor (SMR) technology for merchant marine propulsion," *Ocean Engineering*, vol. 79, pp. 101–130, 2014.

[11] Y. Wu, Z. Chen, L. Hu et al., "Identification of safety gaps for fusion demonstration reactors," *Nature Energy*, vol. 1, pp. 1–11, 2016.

[12] World Nuclear Association, "Nuclear-powered ships," 2017, http://www.world-nuclear.org/info/inf34.html.

[13] World Nuclear News, "Work starts on on-shore infrastructure for Russian floating plant," 2016, http://www.world-nuclear-news.org/WR-Work-starts-on-on-shore-infrastructure-for-Russian-floating-plant-0710165.html.

[14] China Daily, "China to develop floating nuclear power platform in next 5 years," 2017, http://www.chinadaily.com.cn/china/2017-02/14/content_28190934.htm.

[15] IAEA, "Environmental Modelling for Radiation Safety (EMRAS) -a summary report of the results of the EMRAS programme (2003-2007)," IAEA, Vienna, Austria, IAEA-TECDOC-1678, 2012.

[16] L. Monte, P. Boyer, J. E. Brittain et al., "Testing models for predicting the behaviour of radionuclides in aquatic systems," *Applied Radiation and Isotopes*, vol. 66, pp. 1736–1740, 2008.

[17] IAEA, "EMRAS II," 2014, http://www-ns.iaea.org/projects/emras/emras2/default.asp?s=8&l=63.

[18] H. Kawamura, T. Kobayashi, A. Furuno et al., "Preliminary numerical experiments on oceanic dispersion of131I and137Cs discharged into the ocean because of the Fukushima daiichi nuclear power plant disaster," *Journal of Nuclear Science and Technology*, vol. 48, no. 11, pp. 1349–1356, 2011.

[19] Y. Miyazawa, Y. Masumoto, S. M. Varlamov, and T. Miyama, "Transport simulation of the radionuclide from the shelf to open ocean around Fukushima," *Continental Shelf Research*, vol. 50-51, pp. 16–29, 2012.

[20] D. Tsumune, T. Tsubono, M. Aoyama, and K. Hirose, "Distribution of oceanic Cs-137 from the Fukushima Dai-ichi nuclear power plant simulated numerically by a regional ocean model," *Journal of Environmental Radioactivity*, vol. 111, pp. 100–108, 2012.

[21] R. Perianez, I. Brovchenko, C. Duffa et al., "A new comparison of marine dispersion model performances for Fukushima Dai-ichi releases in the frame of IAEA MODARIA program," *Journal of Environmental Radioactivity*, vol. 150, pp. 247–269, 2015.

[22] IAEA, "MODARIA II," 2017, http://www-ns.iaea.org/projects/modaria/modaria2.asp?s=8&l=129.

[23] X. Wu and H. Tang, "Coupling of CFD model and FVCOM to predict small-scale coastal flows," *Journal of Hydrodynamics, Ser. B*, vol. 22, pp. 284–289, 2010.

[24] A. Mazzoldi, T. Hill, and J. J. Colls, "CFD and Gaussian atmospheric dispersion models: a comparison for leak from carbon dioxide transportation and storage facilities," *Atmospheric Environment*, vol. 42, pp. 8046–8054, 2008.

[25] L. Vervecken, J. Camps, and J. Meyers, "Dynamic dose assessment by Large Eddy Simulation of the near-range atmospheric dispersion," *Journal of Radiological Protection*, vol. 35, pp. 165–178, 2015.

[26] OpenFOAM, "The open source CFD toolbox," 2004, http://www.openfoam.com/.

[27] Y. Masumoto, Y. Miyazawa, D. Tsumune et al., "Oceanic dispersion simulations of 137Cs released from the Fukushima daiichi nuclear power plant," *Elements*, vol. 8, pp. 207–212, 2012.

[28] F. Moukalled, L. Mangani, and M. Darwish, *The Finite Volume Method in Computational Fluid Dynamics*, Springer, Berlin, Germany, 2016.

[29] J. H. Ferziger and M. Peric, *Computational Methods for Fluid Dynamics*, Springer, Berlin, Germany, 3rd ed. edition, 2002.

[30] P. Gallagher and R. Marcer, "Best practice guidelines for the application of computational fluid dynamics in marine hydrodynamics," VIRTUE, Europe, VIRTUE - The Virtuel Tank Utility in Europe, 2009.

[31] Z. Warhaft, "Passive scalars in turbulent flows," *Annual Review of Fluid Mechanics*, vol. 32, pp. 203–240, 2003.

[32] I. D. James, "Modelling pollution dispersion, the ecosystem and water quality in coastal waters: a review," *Environmental Modelling & Software*, vol. 17, no. 4, pp. 363–385, 2002.

[33] Y.-H. Koo, Y.-S. Yang, and K.-W. Song, "Radioactivity release from the Fukushima accident and its consequences: a review," *Progress in Nuclear Energy*, vol. 74, pp. 61–70, 2014.

[34] L. Monte, R. Perianez, P. Boyer, J. T. Smith, and J. E. Brittain, "The role of physical processes controlling the behaviour of radionuclide contaminants in the aquatic environment: a review of state-of-the-art modelling approaches," *Journal of Environmental Radioactivity*, vol. 100, pp. 779–784, 2009.

[35] B. Fabritius and G. Tabor, "Improving the quality of finite volume meshes through genetic optimisation," *Engineering with Computers*, vol. 32, no. 3, pp. 425–440, 2016.

[36] F. Flores, R. Garreaud, and R. C. Muñoz, "CFD simulations of turbulent buoyant atmospheric flows over complex geometry: solver development in OpenFOAM," *Computers & Fluids*, vol. 82, pp. 1–13, 2013.